Hexaphosphapentaprismane: A New Gateway to Organophosphorus Cage Compound Chemistry

Mahmoud M. Al-Ktaifani,[d] Walter Bauer,[e] Uwe Bergsträßer,[b] Bernhard Breit,[b, c] Matthew D. Francis,[d] Frank W. Heinemann,[a] Peter B. Hitchcock,[d] Andreas Mack,[b] John F. Nixon,*[d] Hans Pritzkow,[f] Manfred Regitz,*[b] Matthias Zeller,[a] and Ulrich Zenneck*[a]

Dedicated to Professor Walter Siebert on the occasion of his 65th birthday

Abstract: Several independent synthetic routes are described leading to the formation of a novel unsaturated tetracyclic phosphorus carbon cage compound tBu$_4$C$_4$P$_6$ (**1**), which undergoes a light-induced valence isomerization to produce the first hexaphosphapentaprismane cage tBu$_4$C$_4$P$_6$ (**2**). A second unsaturated isomer tBu$_4$C$_4$P$_6$ (**9**) of **1** and the bis-[W(CO)$_5$] complex **13** of **1** are stable towards similar isomerization reactions. Another starting material for the synthesis of the hexaphosphapentaprismane cage tBu$_4$C$_4$P$_6$ (**2**) is the trimeric mercury complex [(tBu$_4$C$_4$P$_6$)Hg]$_3$ (**11**), which undergoes elimination of mercury to afford the title compound **2**. Single-crystal X-ray structural determinations have been carried out on compounds **1**, **2**, **9**, **11**, and **13**.

Keywords: cage compounds · heterocycles · pentaprismanes · phosphorus · strained molecules

[a] Prof. Dr. U. Zenneck, Dr. F. W. Heinemann, Dr. M. Zeller
Institut für Anorganische Chemie
Universität Erlangen-Nürnberg, Egerlandstrasse 1
91058 Erlangen (Germany)
Fax: (+49) 9131-852-7367
E-mail: zenneck@chemie.uni-erlangen.de

[b] Prof. Dr. M. Regitz, Dr. U. Bergsträßer, Prof. Dr. B. Breit
Dr. A. Mack
Fachbereich Chemie der Universität Kaiserslautern
Erwin-Schrödinger-Strasse, 67663 Kaiserslautern (Germany)
Fax: (+49) 631-205-3921
E-mail: regitz@rhrk.uni-kl.de

[c] Prof. Dr. B. Breit
Institut für Organische Chemie, Universität Freiburg
Albertstrasse 21a, 79104 Freiburg (Germany)

[d] Prof. J. F. Nixon, M. M. Al-Ktaifani, Dr. M. D. Francis
Dr. P. B. Hitchcock
School of Chemistry, Physics and Environmental Science
University of Sussex, Brighton, BN1 9QJ (UK)
Fax: (+44) 1273-677196
E-mail: j.nixon@sussex.ac.uk

[e] Priv.-Doz. Dr. W. Bauer
Institut für Organische Chemie
Universität Erlangen-Nürnberg, Henkestrasse 42
91054 Erlangen (Germany)

[f] Dr. H. Pritzkow
Anorganisch-Chemisches Institut, Universität Heidelberg
Im Neuenheimer Feld 270, 69120 Heidelberg (Germany)

Introduction

Cage compounds, especially those which exhibit highly symmetric structures, such as prismane C_6H_6,[1] cubane C_8H_8,[2] or pentaprismane $C_{10}H_{10}$,[3] have always been a subject of interest and fascination for chemists. If one or more of the CH fragments of these molecules are substituted by the isoelectronic P moiety, we enter the field of phosphorus–carbon cage compounds. A recent book gives a comprehensive account of the phosphorus–carbon analogy.[4]

Phosphaalkynes, RC≡P, are ideal starting materials for the formation of organophosphorus cage compounds because of their enormous potential for cycloaddition and cyclooligomerization reactions.[5] For example, thermolysis of *tert*-butylphosphaacetylene tBuC≡P (**3**) leads to six different P–C cage compounds,[6] one of which is the highly symmetrical tetra-*tert*-butyltetraphosphacubane, tBu$_4$C$_4$P$_4$ (**4**). This compound exhibits fascinating spectroscopic and structural features resulting from a unique bonding situation, in which the strong interaction of P lone pair electrons with the P–C σ*-antibonding orbitals of the cube considerably reduces the nucleophilicity of the P atoms.[7]

Phosphaalkynes can be oligomerized with the aid of metal organic reagents or Lewis acids,[8] and the zirconocene-mediated tetramerization of phosphaalkynes is the route of choice for the high-yield preparation of tetraphosphacubane

  0947-6539/02/0811-2622 $ 20.00+.50/0 *Chem. Eur. J.* **2002**, *8*, No. 11

derivatives.[9] Other saturated cage compounds such as pentameric $t\mathrm{Bu}_5\mathrm{C}_5\mathrm{P}_5$[10] and the hexameric $t\mathrm{Bu}_6\mathrm{C}_6\mathrm{P}_6$[11] have been described by us by coupling reactions of the $t\mathrm{Bu}_2\mathrm{C}_2\mathrm{P}_3$ and $t\mathrm{Bu}_3\mathrm{C}_3\mathrm{P}_2$ ring systems, as well as partially unsaturated cages formed by the reaction of highly reactive arene iron(0) complexes with *tert*-butylphosphaalkyne (**3**).[12]

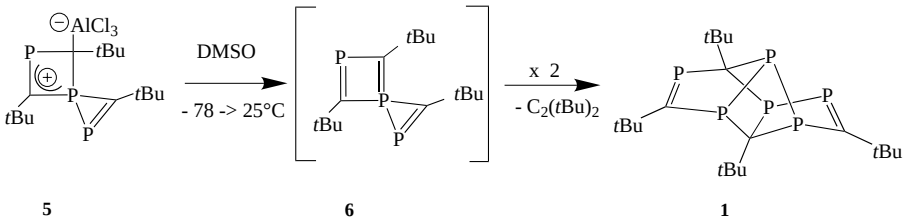

Scheme 1. Formation of tetracyclic $P_6(C{-}t\mathrm{Bu})_4$ cage compound **1**.

Results and Discussion

In this paper we describe the formation of a novel hexaphosphapentaprismane derivative $t\mathrm{Bu}_4\mathrm{C}_4\mathrm{P}_6$ **2**, which can be prepared either by light-induced valence isomerization of an unsaturated precursor $t\mathrm{Bu}_4\mathrm{C}_4\mathrm{P}_6$ **1** or by metal elimination of the remarkable trimeric mercury complex $[(t\mathrm{Bu}_4\mathrm{C}_4\mathrm{P}_6)\mathrm{Hg}]_3$ (**11**). Both **1** and **2** open a new gateway to organophosphorus cage chemistry. They have been synthesized independently by different methods in the laboratories of the authors. In order to prevent unnecessary overlap and duplication of results, we decided to present our results in a single joint publication.

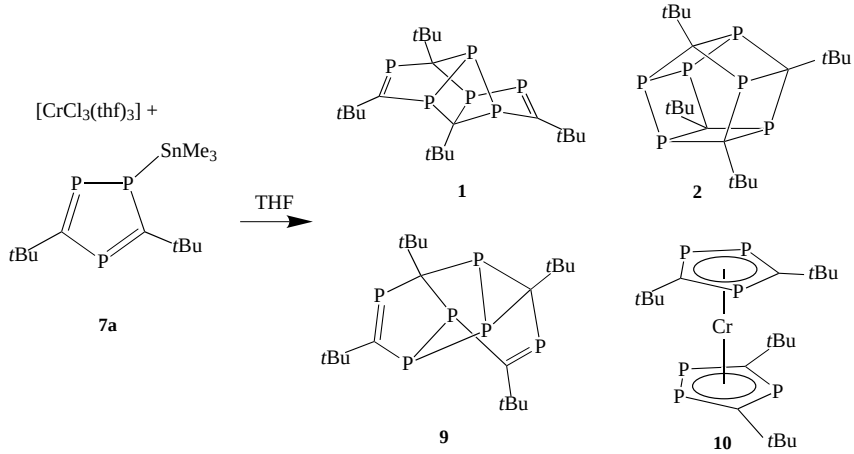

Scheme 2. Treatment of trimethylstannyltriphosphole (**7a**) with an equimolar amount of $[\mathrm{CrCl}_3(\mathrm{thf})_3]$ to give a mixture of several P–C cage compounds with small amounts of **10**.

The first synthetic route is based on the zwitterionic species **5**, the Lewis acidic $AlCl_3$ group of which can be removed by treatment with dimethyl sulfoxide (DMSO) as a Lewis base. The presence of *tert*-butylphosphaalkyne $t\mathrm{BuC}{\equiv}\mathrm{P}$ (**3**) as a trapping reagent leads (depending on the reaction conditions) to the formation of two isomeric phosphaalkyne cyclotetramers each having cage structures.[13] When, however, the spirocyclic zwitterion **5** is treated in the absence of a trapping reagent with an excess of DMSO at $-78\,^{\circ}\mathrm{C}$, the tetracyclic $P_6(C{-}t\mathrm{Bu})_4$ cage compound **1** can be isolated in 22% yield (Scheme 1).

Compound **1** can be viewed as a dimer of the initially formed spirocyclic diphosphete **6**, which has undergone elimination of one molecule of di-*tert*-butylacetylene $t\mathrm{BuC}{\equiv}\mathrm{C}{-}t\mathrm{Bu}$.

The tetracycle **1** is formed more efficiently, however, by reactions utilizing triphospholyl metal complexes such as i) triorganylstannyltriphospholes (**7**)[14] or ii) the potassium salt of 1,2,4-triphospholyl anion (**8**),[15] respectively, as the transfer reagents for the 1,2,4-triphospholyl ring.

Thus treatment of trimethylstannyltriphosphole (**7a**) with an equimolar amount of $[\mathrm{CrCl}_3(\mathrm{thf})_3]$ led to a mixture of several P–C cage compounds together with small amounts of the hexaphosphachromocene (**10**),[16] depending on the reaction conditions employed (Scheme 2).

When the components are reacted for a maximum of two hours, the unsaturated tetracyclic cage compound **1** is the main product and can be isolated in 31% yield by column chromatography. Since the overall composition of cage **1** consists of two neutral 1,2,4-triphospholyl units, a formal coupling of two triphospholyl radicals has taken place, the reaction might involve an electron transfer process.

Interestingly, longer reaction times significantly change the composition of the reaction mixture, and ^{31}P NMR studies monitoring the course of the reaction show that the amount of **1** decreases as new P–C cages are built up; these include both the hexaphosphapentaprismane **2** and a new unsaturated $t\mathrm{Bu}_4\mathrm{C}_4\mathrm{P}_6$ valence isomer **9** (Scheme 2). The pentaprismane $t\mathrm{Bu}_4\mathrm{C}_4\mathrm{P}_6$ (**2**) is most probably formed by a light-induced valence isomerization of **1** (vide infra). The second unsaturated $t\mathrm{Bu}_4\mathrm{C}_4\mathrm{P}_6$ isomer **9** can be readily isolated by chromatographic workup as a mixture with hexaphosphachromocene (**10**), which is not easy to separate. No NMR signals for **10** are observable owing to its paramagnetism, thus no accurate determination of the yield of **9** can be given. Compound **9** contains only one 1,2,4-triphospholene ring, which can be readily traced back to the starting material **7a**, thus indicating a complex rearrangement reaction, the mechanism of which is not yet clear.

The unsaturated compound **1**, which is red, readily undergoes a light-induced valence isomerization and on exposure to visible light, even diffuse daylight is sufficient, rearranges to form the hexaphosphapentaprismane cage (**2**) in about 40% yield (Scheme 3).

In contrast to **1**, bright yellow isomer **9**, however, does *not* undergo a similar isomerization to form the title compound **2**.

Better yields of **1** and/or **2** can be achieved by the reaction of **7a** or **8** with mercury(II) chloride followed by the

  0947-6539/02/0811-2623 $ 20.00+.50/0

degradation of the intermediate triphospholyl mercury compounds. Thus, when two equivalents of $[K(tBu_2C_2P_3)]$ were treated with one equivalent of $HgCl_2$ in THF, under the influence of daylight a yellow suspension developed over a 24 h period, and after longer stirring precipitation of elemental mercury resulted together with the formation of an orange solution. Hexaphosphapentaprismane $tBu_4C_4P_6$ (**2**) can be obtained in about 20% yield by extracting with toluene and keeping this solution at $-25\,^{\circ}C$ for a further 24 h (Scheme 4).

Although, like the method utilizing chromium(III) and stannyltriphosphole **7a**, the hexaphosphapentaprismane $tBu_4C_4P_6$ (**2**) was clearly formed by an overall coupling of two $tBu_2C_2P_3$ fragments, but in this case the reaction pathway appeared to involve other intermediates, and the reaction was investigated more thoroughly. When the reaction of $[K(tBu_2C_2P_3)]$ and $HgCl_2$ was stopped after about 10 h, the yellow suspension mentioned above could be isolated and identified as a remarkable trimercury cluster compound $[(tBu_4C_4P_6)Hg]_3$ (**11**) (45% yield, Scheme 5).

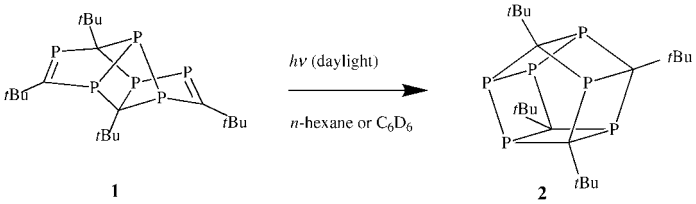

1 **2**

Scheme 3. Light-induced valence isomerization of compound **1** and rearrangement to form **2**.

^{31}P NMR spectroscopic studies on reaction mixtures suggest that other oligomers of the type $[(tBu_4C_4P_6)Hg]_n$ may also be present in solution, but the compounds have not yet been isolated. When a solution of **11** is put aside for a few hours, elemental mercury begins to precipitate. As the pentaprismane substructure is already preformed in **11** a direct elimination of the metal occurs with no signs from NMR spectroscopy of any intermediates.

However, when $HgCl_2$ is treated with stannyltriphosphole **7a** in diethyl ether, not the trimercury complex **11** but a compound **12** can be isolated in almost quantitative yield, which we believe to be bis(η^1-1,2,4-triphospholyl)mercury. It is a dark red amorphous solid, which is stable in air and moisture resistant. In contrast to this remarkable stability, it decomposes rapidly when brought into contact with nonpolar solvents like *n*-hexane or toluene. The unsaturated PC cage **1** is formed this way in good yield together with metallic mercury. Compound **12** has been proven to be insoluble in any solvent tested so far, and thus no solution spectra are available. ^{31}P NMR CPMAS spectra of the solid exhibit two isotropic signals at $\delta = 295$ and 161, respectively. This may be interpreted as a hint to a symmetrical bonding mode of the triphospholyl ligand or a rapid exchange process in the solid state. Assuming a linear coordinated mercury(II) center as the basic structural feature and a corresponding metal–ligand bonding situation as for the stannyl compounds **7**, we found that a fluxional Hg–P bond in the solid state would explain the experimental findings best. One possible explanation is a fast 1,5-sigmatropic shift of the Hg atom between the two neighboring phosphorus atoms (Scheme 6). The activation barrier for such a process can be as small as the 31 kJ mol^{-1} we determined for 1-triphenylstannyl-1,2,4-triphosphole **7b**.[14]

The insolubility of **12**, even in coordinating solvents such as THF, acetone, or water, is surprising. A possible explanation may be a significant interaction of the Lewis acidic mercury atom with the triphospholyl ligands of an other molecule and the formation of a polymeric structure. This would result in an increase of the coordination number of the Hg atom and a bent P–Hg–P interaction, but it is compatible with the spectroscopic results for **12**. A polymeric chain structure has been reported recently for bis(triphospholyl)strontium in the solid state.[17]

8 **2**

Scheme 4. Formation of hexaphosphapentaprismane $tBu_4C_4P_6$ (**2**).

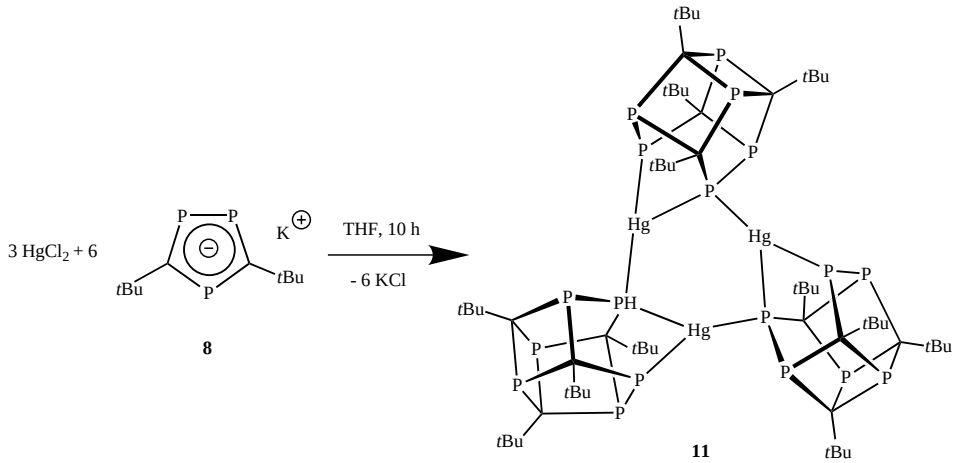

8 **11**

Scheme 5. Formation of trimercury cluster compound $[(tBu_4C_4P_6)Hg]_3$ (**11**) after the reaction of $[K(tBu_2C_2P_3)]$ and $HgCl_2$.

The formation of the two mercury triphospholyl complexes **11** and **12** with the same empirical formula but different states of aggregation is somehow surprising and cannot be fully explained at the moment. The main difference between both starting materials stannyltriphosphole **7a** and triphospholyl potassium **8** is the coordination mode of the metal and the formal charge of the ring. While in **7a** the tin atom is

  0947-6539/02/0811-2624 $ 20.00+.50/0 *Chem. Eur. J.* **2002**, *8*, No. 11

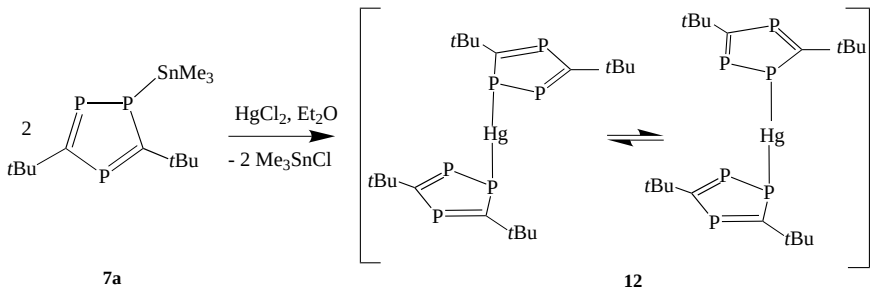

Scheme 6. Formation of bis(triphospholyl)mercury (**12**).

fluxionally η^1-coordinated to a neutral ring, in **8** the potassium cation is mainly electrostatically attached to the aromatic triphospholyl anion. Since both the synthesis of **11** and **12** have been carried out in donor solvents like Et_2O and THF, a stabilization of a possible bis(triphospholyl)mercury compound by the ether seems to be of minor importance. Interestingly, when the reaction of $[K(tBu_2C_2P_3)]$ and $HgCl_2$ is carried out in the dark, no formation of **11** is observed. This is a clear hint towards a photochemically initiated formation of **11**. In contrast to that, no signs for a formation of the trimeric mercury complex **11** are found when the reaction of stannyltriphosphole **7a** and $HgCl_2$ is carried under the influence of daylight.

When the reaction of $HgCl_2$ and stannyltriphosphole **7a** is carried out in toluene, **12** is not isolable but decomposes almost immediately. After separation of elemental mercury from the reaction mixture, **1** can be isolated in a yield of 72% (Scheme 7).

While for the reaction of **7a** with chromium(III) the formation of **1** occurs most probably by an oxidative coupling of the triphospholyl units, this appears not to be the case for bis(triphospholyl)mercury (**12**). Its degradation reaction seems to be somewhat autocatalytic. After an induction period without any visible decay, the reaction starts at some randomly appearing pale gray points. These regions of mercury formation rapidly expand until all **12** is consumed. We take this as a hint to a chain reaction, and, with mercury being involved, a radical chain mechanism is very likely.

As observed for **12**, some other main group bis(triphospholyl) complexes exhibit a tendency towards reductive elimination of the metal, for example, although the bis(1,2,4-triphospholyl) complexes of lead(II) and tin(II) are moderately stable, under the influence of light, or even during workup they often undergo decomposition.[18] The corresponding diphosphastibolyl derivatives are even more unstable, and attempts to synthesize metal π complexes of these ring anions resulted in the formation of a PSbC cage compound, which is isostructural with **1**.[19]

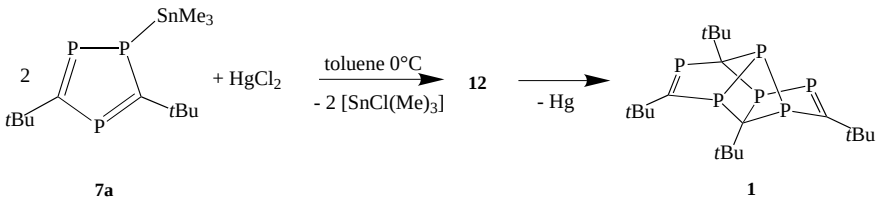

Scheme 7. Formation of **1** via **12**.

Structural and NMR spectroscopic studies: All the $tBu_4C_4P_6$ valence isomers **1**, **2**, and **9** as well as the trimeric mercury complex **11** have been studied by X-ray crystallography (Figures 1, 2, 3, and 4, and Tables 1, 2, 3, 4, 5, and 6). The three cages are chiral and contain several stereogenic centers but only one pair of enantiomers is observable in the solid state.

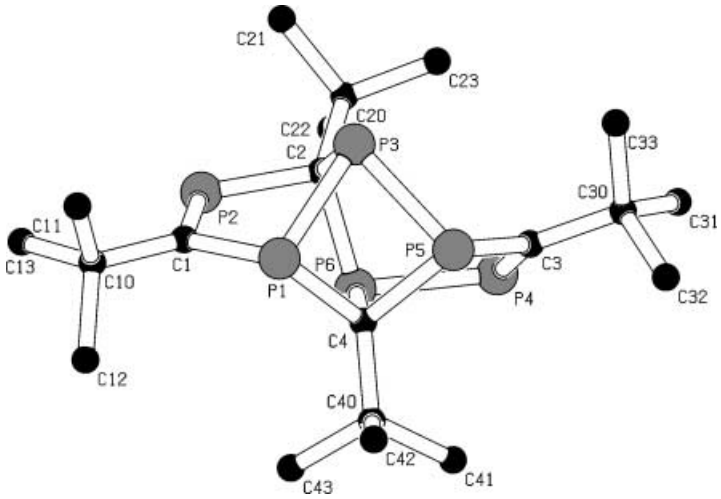

Figure 1. Molecular structure of **1** in the solid state; hydrogen atoms are omitted for clarity.

Compound **1** crystallizes in the non-centrosymmetric space group $Pca2_1$, and both enantiomeric crystal forms are present. The unit cell contains two crystallographically independent molecules of one enantiomer, which are structurally almost identical.

Compound **9** exhibits crystals belonging to the triclinic space group $P\bar{1}$. Again, both enantiomeric forms are present in the unit cell. The two P–C cage compounds **1** and **9** differ from **2** in that they are both unsaturated and each contain two phosphorus carbon double bonds.

The smallest cyclic unit of **1** is a four-membered P_3C ring, having a typical "envelope" structure. In line with this, the bond angles within the four-membered cycle are all below 90° and are 74.4(1) to 82.7(2)° at phosphorus and 89.5(3)° at carbon. From a general point of view, **1** can be regarded as a dimer of 1,2,4-triphospholyl rings, which have been split into separate diphosphaallyl and P=C double bond π systems. The formal dimerization occurs by the connection of the P1–P3–C2 and P5–C4–P6 diphosphaallyl subunits by three single bonds, and the P=C double bonds remain unaffected. The bond lengths within the two five-membered rings are unexceptional, whereas, both

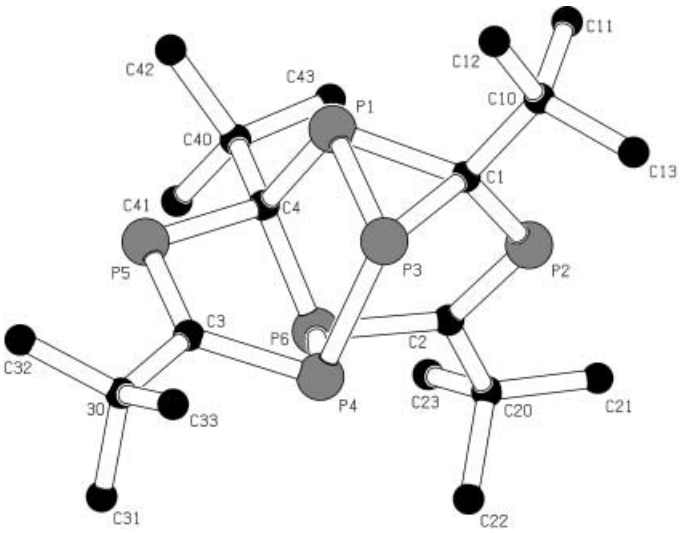

Figure 2. Molecular structure of **9** in the solid state; hydrogen atoms are omitted for clarity.

the bridging P–P bonds as well as the P–C bonds are remarkably long. The bond length P3–P5 is 2.243(3) Å, which is in the upper range observed for P–P single bonds,[20] and the bonds P1–C4 and C2–P6 are 1.921(8) and 1.908(8) Å, respectively. It appears that the linkage between the two triphospholyl units in **1** is somewhat strained and thereby contributes to its ready rearrangement.

The second tBu$_4$C$_4$P$_6$ isomer **9** exhibits a three-membered P_2C ring as the smallest cyclic unit. The interior angles of this three-membered ring are 55.66(8) and 54.75(7)° at phosphorus and 69.60(8)° at carbon. In contrast to **1**, all bond lengths

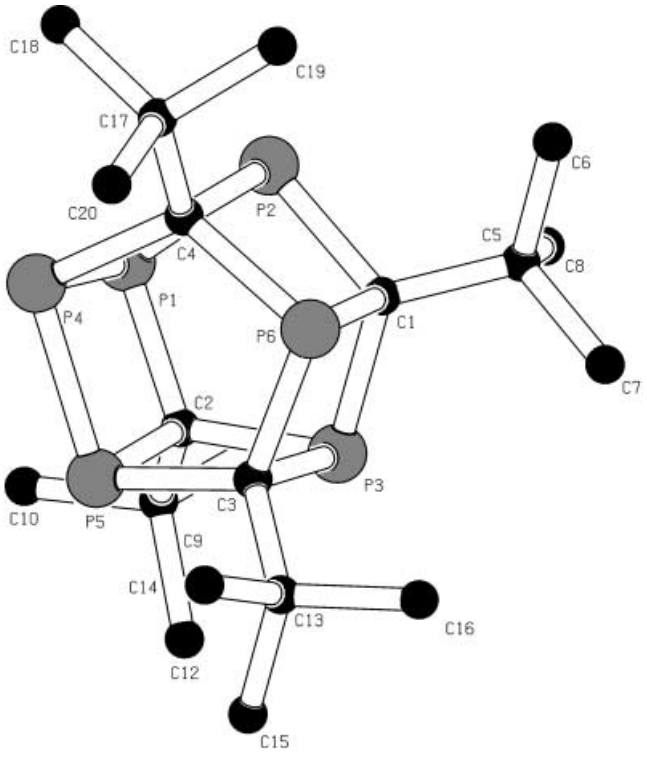

Figure 3. Molecular structure of **2** in the solid state; hydrogen atoms are omitted for clarity.

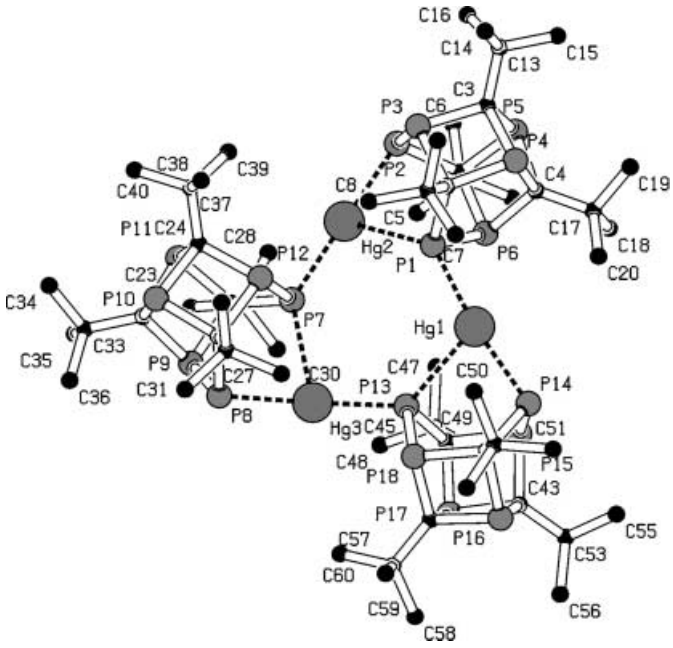

Figure 4. Molecular structure of **11** in the solid state; hydrogen atoms are omitted for clarity.

Table 1. Selected bond lengths [Å] and angles [°] for **1**.

P2–C1	1.645(9)	P6–C2	1.908(8)
P4–C3	1.686(8)	P1–C4	1.921(8)
P1–P3	2.203(3)	P1–C1–P2	118.0(5)
P4–P6	2.223(3)	P4–C3–P5	119.5(4)
P3–P5	2.243(3)	P1–P3–P5	74.4(1)
P1–C1	1.855(9)	P3–P5–C4	82.1(3)
P2–C2	1.871(8)	C4–P1–P3	82.7(2)
P5–C3	1.823(8)	P5–C4–P1	89.5(3)
P5–C4	1.897(7)	P5–C4–P6	104.7(3)
P6–C4	1.874(8)	P1–C4–P6	110.7(4)

Table 2. Selected bond lengths [Å] and angles [°] for **9**.

P2–C2	1.674(2)	P4–C3	1.853(2)
P5–C3	1.683(2)	P6–C2	1.817(2)
P6–P4	2.183(1)	P2–C1	1.820(2)
P4–P3	2.227(1)	P1–P3–C1	54.75(7)
P3–P1	2.163(1)	P3–P1–C1	55.66(8)
P1–C1	1.884(2)	P1–C1–P3	69.60(8)
P3–C1	1.905(2)	P2–C2–P6	125.8(2)
P5–C4	1.897(2)	P4–C3–P5	119.4(2)

Table 3. Selected bond lengths [Å] and angles [°] for **2**.

P1–P2	2.218(1)	P2–C1–P3	117.31(9)
P4–P5	2.221(1)	C1–P3–C2	103.41(8)
P1–P4	2.282(1)	P3–C2–P1	116.55(9)
C1–P2	1.880(2)	C2–P1–P2	101.01(6)
C1–P3	1.873(2)	P4–P5–C3	101.44(6)
C2–P3	1.877(2)	P5–C3–P6	117.18(9)
C2–P1	1.887(2)	C3–P6–C4	103.34(8)
C3–P5	1.878(2)	P6–C4–P4	116.94(9)
C3–P6	1.873(2)	C4–P4–P5	100.27(6)
C4–P6	1.876(2)	P2–C1–P6	92.22(8)
C4–P4	1.898(2)	P3–C1–P6	92.18(8)
C1–P6	1.913(2)	P2–C4–P4	100.39(8)
C2–P5	1.907(2)	C1–P2–C4	87.06(8)
C3–P3	1.903(2)	C1–P3–C3	87.54(8)
C4–P2	1.913(2)	C4–P4–P1	87.96(6)
P1–P2–C1	100.87(6)	P2–P1–P4	81.14(2)

  0947-6539/02/0811-2626 $ 20.00+.50/0 *Chem. Eur. J.* **2002**, *8*, No. 11

Table 4. Selected bond lengths [Å] and angles [°] for **11**.

Hg1–P1	2.436(2)	Hg3–P7	2.865(2)
Hg2–P12	2.431(2)	P14–Hg1–P13	79.13(5)
Hg3–P13	2.423(2)	P1–Hg2–P2	79.67(5)
Hg1–P14	2.448(2)	P7–Hg3–P8	79.12(5)
Hg1–P13	2.811(2)	P1–Hg1–P14	171.13(6)
Hg2–P2	2.442(2)	P2–Hg2–P7	173.43(6)
Hg2–P1	2.821(2)	P8–Hg3–P13	163.31(6)
Hg3–P8	2.436(2)		

Table 5. Crystal data and structure refinement of **1**[a] and **9**.

	1	**9**
empirical formula	$C_{20}H_{36}P_6$	$C_{20}H_{36}P_6$
M_r	462.31	462.31
solvent	*n*-hexane	*n*-hexane
crystals	orange plate	yellow fragment
T [K]	200(2)	200(2)
crystal system	orthorhombic	triclinic
space group	$Pca2_1$	$P\bar{1}$
unit cell dimensions a [Å]	20.698(3)	10.050(1)
b [Å]	12.738(4)	11.118(1)
c [Å]	18.832(2)	12.003(2)
α [°]	90	92.37(1)
β [°]	90	102.43(1)
γ [°]	90	104.83(1)
V [Å]	4965.1(18)	1259.5(3)
Z	8	2
ρ_{calcd} [g cm^{-3}]	1.237	1.219
μ [mm^{-1}]	0.437	0.431
$F(000)$	1968	492
crystal size [mm]	0.9 × 0.4 × 0.08	0.60 × 0.40 × 0.30
θ range [°]	1.85–27.00	1.90–27.00
index ranges	$-1 \le h \le 26$	$-12 \le h \le 1$
	$-1 \le k \le 16$	$-13 \le k \le 14$
	$-1 \le l \le 24$	$-15 \le l \le 15$
reflns collected	6797	6445
independent reflns	5918 [$R_{int} = 0.0327$]	5486 [$R_{int} = 0.0264$]
reflns [$I > 2\sigma(I)$]	4384	4268
completeness to $\theta = 27.0°$ [%]	99.9	99.8
absorption correction	ψ scan	none
max. and min. transmission	0.5165/0.4485	–
refinement method	full-matrix least-squares on F^2	
data/restraints/parameters	5918/1/470	5486/0/343
goodness-of-fit on F^2	1.016	1.012
final R indices [$I > 2\sigma(I)$] $R1$	0.0649	0.0418
$wR2$	0.1526	0.0956
R indices (all data) $R1$	0.0962	0.0603
$wR2$	0.1723	0.1038
largest diff. peak hole [e Å^{-3}]	1.131/–0.430	0.527/–0.320

[a] The unit cell of **1** contains two crystallographically independent molecules of one enantiomer, which are structurally almost identical. The measured crystal was an inversion twin, the domain proportions had been approximately 50%.

lie in the expected range, and there is no sign of strain in the molecule.

The third tBu$_4$C$_4$P$_6$ isomer hexaphosphapentaprismane **2** crystallizes in the monoclinic space group $P2_1/c$. As for the other cages, both enantiomeric forms are present in the unit cell. In the crystal the molecule slightly deviates from the expected C_2 symmetry.

As for its precursor **1**, compound **2** is a strained molecule. The P–C and the P–P bond lengths can be divided into two groups. The bond lengths in the five-membered rings lie in the range expected for P–C and P–P single bonds,[20] whereas the other skeletal bonds, which connect the two five-membered rings by generating five four-membered rings, are surprisingly long. The mean P–C bond length of those bonds is 1.880 Å, and the bond length P1–P4 is 2.282(1) Å. P–P single bond lengths of this size are very rare and have not been previously observed within P–C cage compounds. Comparable values have been found only for some allotropes of phosphorus[21] or in certain polyphosphorus compounds.[22]

The bond angles within the two five-membered rings lie between 100.27(6) and 103.34(8)° at phosphorus and 116.55(9) and 117.18(9)° at carbon, respectively. The deviation from the ideal five-membered ring value of 109° is significant, but agrees well with the findings for other P–C heterocycles and results from the different sizes of the two atoms in these types of compounds. On the other hand, the interior angles of the four-membered rings correspond very closely to the pentaprismane basic structure; the CPC angles are a little below 90° (87.10(8) to 89.46(5)°), and the PCP angles are slightly above this value (92.18(8) to 92.50(8)°). The deviation from the idealized value is even smaller than previously observed for tetraphosphacubane **4**, another sign for the concentration of the molecular strain in the bonds which connect the five-membered 1,2,4-triphospha rings. Due to the fixed pentaprismane structure, which is constructed of building blocks of different size, the atoms of the P_4 chain P2–P1–P4–P5 are squeezed slightly out of the cage, and the PPP angles are reduced to 80.66(2) and 81.14(2)°, respectively.

According to detailed theoretical calculations, the pentaphosphaprismane cage **2** represents a molecule, the reactivity of which is likely to be associated mainly with the unique P–P bond linking the two five-membered 1,2,4-triphospholane subunits, and in support of this thesis, **2** readily reacts with S, Se, and Te at this P–P bond to quantitatively afford new cage molecules of the type EC$_4$$tBu_4P_6$ (E = S, Se, Te).[23]

A single-crystal X-ray diffraction study reveals the remarkable structure of **11** in the solid state (Figure 4, Table 4, and Table 6), which consists of three HgC$_4$$tBu_4P_6$ units; each unit is linked to the other two by coordinative bonds from phosphorus lone pairs.

In each individual HgC$_4$$tBu_4P_6$ unit the two C$_2$$tBu_2P_3$ rings are linked together, as a result of an internal cycloaddition reaction, in such a way that each P atom from one ring is bonded to a C atom of the other ring, while the Hg atom bridges the two remaining phosphorus atoms. Within each HgP$_6$C$_4$$tBu_4$ unit, the mean Hg–P($\lambda^3\sigma^3$) bond length is 2.4421 Å, which is significantly shorter than the mean Hg–P($\lambda^3\sigma^4$) bond length (2.8321 Å), and the mean P–Hg–P angle is 79.30°. The three HgC$_4$$tBu_4P_6$ units are linked in a way resulting in a distorted hexagon [Hg1–P1–Hg2–P7–Hg3–P13]; the mean Hg–P–Hg angle is 131.40°, whereas the mean P–Hg–P angle is 105.09° within the hexagon. In the HgC$_4$$tBu_4P_6$ trimer, the mean P($\lambda^3\sigma^3$)–Hg–P′($\lambda^3\sigma^4$) angle is very close to linearity (169.29°). Not surprisingly the bond lengths (C–P and P–P) within each unit of the trimer **11** do not differ remarkably from the corresponding values found in the hexaphosphapentaprismane **2**.

All NMR data of the cage compounds **1**, **2**, and **9** as well as those of trimercury complex **11** are in line with the structural findings for the crystalline material. The C_1-symmetric

Table 6. Crystal data and structure refinement of **2** and **11**.[a]

	2	**11**
empirical formula	$C_{20}H_{36}P_6$	$C_{66}H_{128}Hg_3O_2P_{18}$
M_r	462.31	2136.93
solvent	*n*-hexane	diethyl ether
crystals	orange fragment	yellow prism
T [K]	173(2)	173(2)
crystal system	monoclinic	monoclinic
space group	$P2_1/c$	$P2_1/c$
unit cell dimensions a [Å]	10.5672(6)	14.7235(3)
b [Å]	10.3418(5)	28.4257(7)
c [Å]	22.505(1)	22.0497(3)
α [°]	90	90
β [°]	100.053(1)	103.680(2)
γ [°]	90	90
V [Å^3]	2421.7(2)	8966.6(3)
Z	4	4
ρ_{calcd} [g cm^{-3}]	1.268	1.583
μ [mm^{-1}]	0.448	5.483
$F(000)$	984	4248
crystal size [mm]	0.32 × 0.08 × 0.07	0.30 × 0.20 × 0.10
θ range [°]	1.84 – 28.29	3.71 – 25.02
index ranges	$-14 \le h \le 13$	$-17 \le h \le 16$
	$0 \le k \le 13$	$-27 \le k \le 33$
	$0 \le l \le 29$	$-26 \le l \le 24$
reflns collected	16658	39454
independent reflns	5858 [$R_{int} = 0.039$]	15548 [$R_{int} = 0.057$]
reflections [$I > 2\sigma(I)$]	4318	12397
completeness to $\theta = 28.29°$ [%]	97.4	98.2
absorption correction	semi-empirical from multiscan equivalents	
max./min. transmission	0.928/0.773	0.383/0.314
refinement method	full-matrix least-squares on F^2	full-matrix least-squares on F^2
data/restraints/parameters	5858/0/379	15548/0/782
goodness-of-fit on F^2	0.933	1.099
final R indices [$I > 2\sigma(I)$] $R1$	0.0323	0.0480
$wR2$	0.0693	0.1012
R indices (all data) $R1$	0.0534	0.0673
$wR2$	0.0745	0.1085
largest diff. peak hole [e Å^{-3}]	0.567/ – 0.247	1.405/ – 1.433

[a] In the unit cell of **11** there are two ether solvate molecules, one ordered and the other disordered, which were approximated by including eight carbon atoms at ½ occupancy.

molecules **1** and **9** exhibit four ^{1}H NMR signals and six ^{31}P NMR resonances. Each two of the ^{31}P NMR signals appear at very low field around $\delta = 300$ and can be assigned to the P=C double bonds. The other four ^{31}P NMR signals of **1** are located between $\delta = 32$ and -13. Compound **9** exhibits one signal at $\delta = 23$, and the three remaining ones are located between $\delta = -113.5$ and -124.4. Such high field resonances are regularly observed for P atoms as parts of three-membered rings.[24] The coupling patterns of both **1** and **9** are in full accord with their solid-state structures. In the case of **1** three J_{PP} coupling constants of the four-membered ring P1–P3–P5–C4 exhibit values, which are regarded as characteristic for $^1J_{PP}$ coupling constants (131, 149, and 187 Hz). However, one of them must be a $^2J_{PP}$. Due to the folding of the ring, the orientation of the lone pairs of P1 and P5 is close to parallel and allows a strong interaction between these two nuclei, which explains the surprisingly high ^2J coupling constant. A comparable observation is made in the ^{31}P NMR spectrum of **9** for the ^3J coupling between P2 and P4 across a six-membered ring. The value of 19.7 Hz is markedly high and can be explained by the interaction of the lone pair of P4 with the π system of the P=C double bond, which are directing towards each other.

C_2-symmetric **2** exhibits only two ^{1}H and three ^{31}P NMR signals. The ^{31}P NMR resonance of the P_2 bridge P1–P4 appears at $\delta = -3.8$, and the other two signals are detected at surprisingly low field for $\lambda^3\sigma^3$ phosphorus atoms (P2, P5: $\delta = 178.1$; P3, P6: $\delta = 241.9$). As for tetraphosphacubanes, these unusual ^{31}P NMR positions are a hint to a strong participation of the P lone pairs in the P–C σ* orbitals of the cage.[7]

The ^{31}P coupling pattern of **2** has been fully analyzed by iterative spectrum simulation (Figure 5 and Table 7). The ^1J coupling constants are opposite in sign, and their numeric values are 63.7 and 86.4 Hz. The range of $^1J_{PP}$ coupling constants includes values from -620 to $+800$ Hz. The $\lambda^3\sigma^3$ phosphorus atoms are generally associated with negative values of three figure numbers,[25] thus a surprising shift towards positive numbers can be stated. As for the unusual ^{31}P NMR resonance positions, this may be related to the strong participation of the phosphorus lone pairs in the P–C σ bonds.

As the signs of the coupling constants cannot be determined directly from the ^1J values, the ^2J coupling constants are utilized instead. Two of the ^2J coupling constants are relatively high, and their numeric values are 33.3 and 29.6 Hz. Since

  0947-6539/02/0811-2628 $ 20.00+.50/0 *Chem. Eur. J.* **2002**, *8*, No. 11

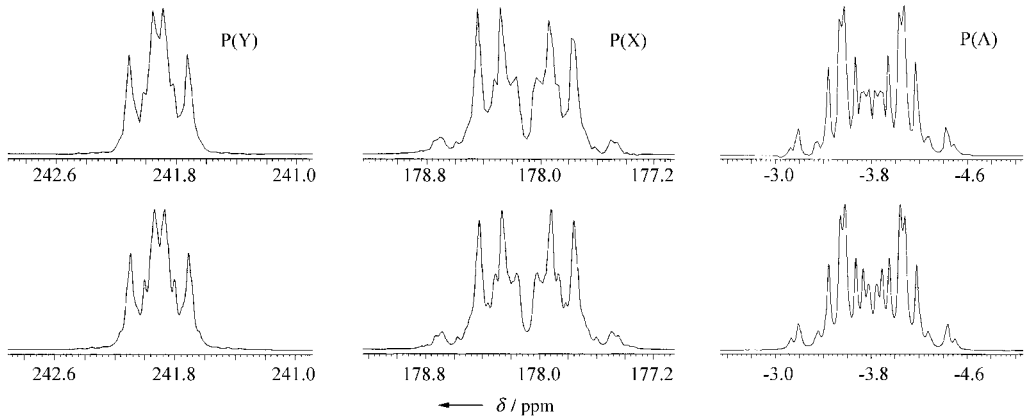

Figure 5. Experimental (upper part: 161.7 MHz, $CDCl_3$, 24.7 °C) and simulated (lower part) $^{31}P\{^1H\}$ NMR spectra of **2**. Data see Table 7.

Table 7. ^{31}P NMR coupling constants of **2**.

	Y′	Y	X′	X	A′
A	3.56	33.33	4.46	– 86.42	63.74
X	29.55	– 3.80	5.99		
Y	– 6.74				

such coupling constants are in most cases positive,[25] all signs are assigned according to this (Table 7).

In contrast to the parent pentaprismane **2**, the trimeric mercury compound **11** lacks C_2 symmetry, and as a consequence six phosphorus resonances are seen (Figure 6) instead

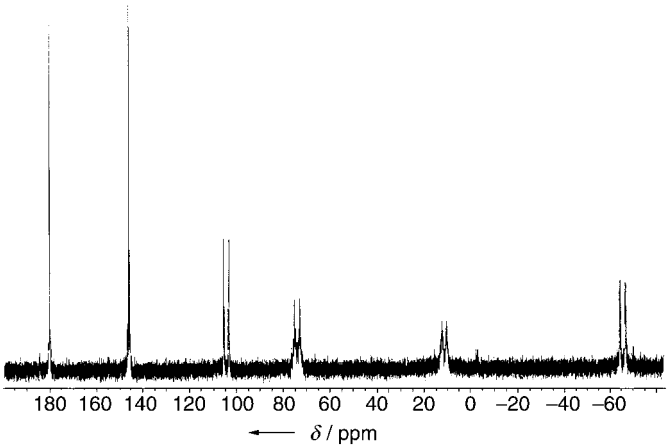

Figure 6. $^{31}P\{^1H\}$ NMR spectrum of $[(t\mathrm{Bu}_4\mathrm{C}_4\mathrm{P}_6)\mathrm{Hg}]_3$ (**11**) (121.68 MHz, $CDCl_3$, 25 °C).

of the three observed in **2** (Figure 5). The six resonances can all be assigned (see Experimental Section for details), and they are all complex multiplets, however the large $^1J_{PP}$ coupling constants can be readily identified in each of the four resonances corresponding to those phosphorus centers, which are singly bonded to another phosphorus atom in the cage. These couplings, which are 269 and 285 Hz, respectively, are quite typical for $^1J_{PP}$ coupling constants.

The light-induced valence isomerization of **1** can be blocked by σ complexation to tungsten pentacarbonyl fragments. If **1** is treated with two equivalents of $[W(CO)_5(thf)]$, the bis(pentacarbonyltungsten) complex **13** is formed and can be isolated in 46 % yield (Scheme 8).

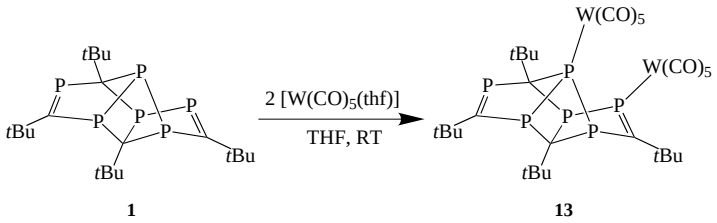

Scheme 8. Treatment of **1** with two equivalents of $[W(CO)_5(thf)]$ to give bis(pentacarbonyltungsten) complex **13**.

Compound **13** has been fully characterized including multinuclear NMR and X-ray structural analysis. It crystallizes in the monoclinic space group $P2_1/n$ (Figure 7 and Tables 8 and 9).

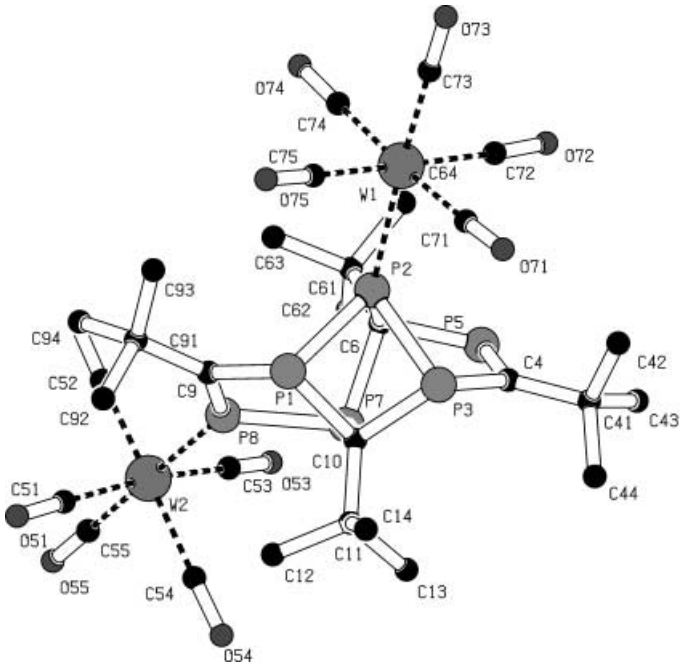

Figure 7. Molecular structure of **13** in the solid state; hydrogen atoms are omitted for clarity.

Table 8. Selected bond lengths [Å] and angles [°] for **13**.

W1–P2	2.544(2)	P7–C6	1.922(5)
W2–P8	2.501(2)	P3–C10	1.921(5)
P8–C9	1.679(6)	C9–P8–W2	138.1(2)
P5–C4	1.681(7)	P7–P8–W2	119.67(7)
P3–P2	2.192(2)	C9–P8–P7	101.5(2)
P2–P1	2.240(2)	C4–P5–C6	101.5(3)
P7–P8	2.222(2)	P8–C9–P1	115.4(3)
P3–C4	1.834(6)	P5–C4–P3	118.1(3)
C10–P7	1.871(5)	P3–P2–P1	75.59(7)
C10–P1	1.893(5)	C10–P3–P2	81.7(2)
P5–C6	1.886(6)	C10–P1–P2	81.0(2)
C6–P2	1.899(6)	P1–C10–P3	90.8(2)
C9–P1	1.830(6)	P7–C10–P1	105.2(3)

Table 9. Crystal data and structure refinement of **13**.

	13
empirical formula	$C_{30}H_{36}O_{10}P_6W_2$
M_r	1110.11
solvent	*n*-pentane
crystals	orange red fragment
T [K]	293(2)
crystal system	monoclinic
space group	$P2_1/n$
unit cell dimensions a [Å]	11.067(2)
b [Å]	21.731(4)
c [Å]	17.776(4)
α [°]	90
β [°]	108.11(3)
γ [°]	90
V [Å^3]	4063.0(14)
Z	4
ρ_{calcd} [g cm^{-3}]	1.815
μ [mm^{-1}]	5.942
$F(000)$	2136
crystal size [mm]	0.35 × 0.25 × 0.20
θ range [°]	2.15 – 26.06
index ranges	$-12 \le h \le 12$ $-26 \le k \le 26$ $-21 \le l \le 21$
reflns collected	42675
independent reflns	7626 [$R_{int} = 0.1333$]
reflns [$I > 2\sigma(I)$]	6587
refinement method	full-matrix least-squares on F^2
data/restraints/parameters	7626/0/433
goodness-of-fit on F^2	0.994
final R indices [$I > 2\sigma(I)$] $R1$	0.0468
$wR2$	0.1189
R indices (all data) $R1$	0.0538
$wR2$	0.1284
largest diff. peak hole [e Å^{-3}]	2.293 – 1.574

As one would suppose, the complexation of the cage does not change the structural and spectral parameters of **1** dramatically. The differences between **13** and **1** are clearly due to interaction of the lone pairs of P3 and P4 with the metal atoms, and the interaction does not interfere significantly with the framework of the P–C skeleton. Therefore the stabilization effect of the [W(CO)$_5$] fragments is probably due to the increase of a sterically crowded situation at the surface of the cage structure. The P–W distances are in the typical range of those evaluated for comparable compounds.[26]

During the rearrangement of **1** into **2** two P=C double bonds are replaced by four P–C single bonds, and the number of P–P bonds is constant. As for more simple types of phosphaalkenes, the formation of saturated follow-up products is the thermodynamically favored process. Since visible light of low intensity is sufficient to initiate the isomerization reaction, a photochemical activation seems to be the key step. We assume that the absorption of a photon causes the homolysis of an appropriate bond of the molecule. Bond strength, radical stabilization, and reduction of molecular strain lead us to assume that the bond P3–P5 is broken. Biradical **1a** would be the short-lived primary product of the process (Scheme 9).

To find evidence for this hypothesis, photolysis experiments with **1** have been done under EPR spectroscopic control. If **1** is exposed to daylight in nonpolar solvents like *n*-hexane or toluene, a doublet radical **1b** can be detected ($\langle g \rangle = 2.013$). It exhibits strong coupling with six inequivalent ^{31}P nuclei, and the coupling pattern has been determined by spectrum simulation (Figure 8).

By irradiation of solutions of **1** in hexane with a 75 W xenon short cut lamp, the signal of **1b** gets stronger, and after two hours a maximal intensity is reached (ca. nine times the starting value). Then the intensity stays almost constant for several hours. Compound **1b** can be detected even after storing samples for one week at $-30\,^{\circ}$C in the dark. As the spectral parameters of **1b** exclude a biradical, and due to its long lifetime, **1b** cannot be identical with **1a**, but is believed to be a consecutive product, for which a localized radical function of biradical **1a** abstracted a hydrogen atom from the solvent (Scheme 9). This process competes with the rearrangement **1** → **1a** → **2**, and the complete consumption

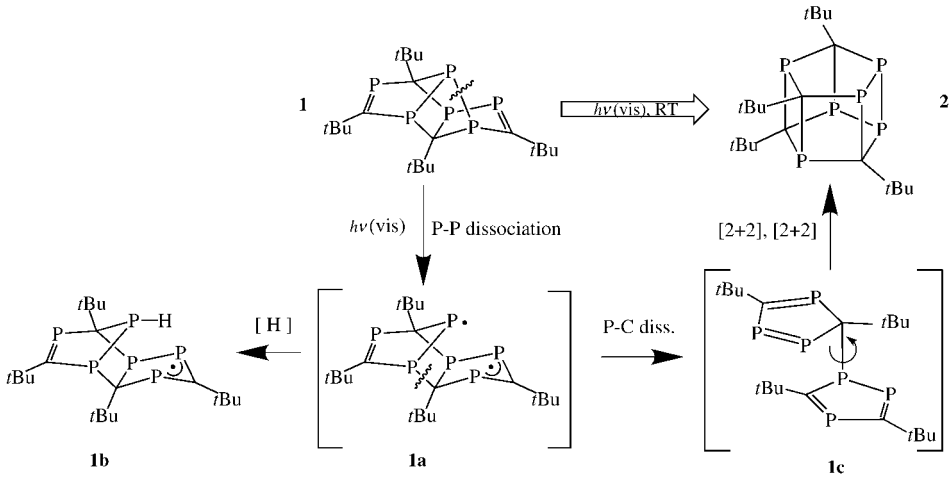

Scheme 9. Initial photochemical P–P bond breaking, a P–C bond dissociation, and a radical recombination reaction can form a closed-shell intermediate **1c**. This can undergo a twofold [2+2] cyclic addition reaction to give hexaphosphapentaprismane (**2**).

  0947-6539/02/0811-2630 $ 20.00+.50/0 *Chem. Eur. J.* **2002**, *8*, No. 11

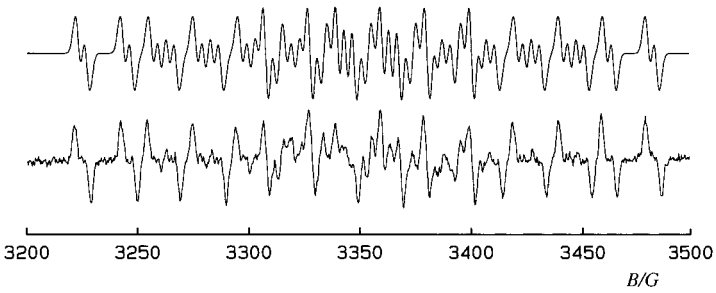

Figure 8. EPR spectrum of the doublet radical **1b**, which is formed by photolysis of **1** in *n*-hexane (xenon short cut lamp, 120 min, 75 W). Lower part: experimental spectrum (9.45 GHz, 2.01 mW, 0.2 G modulation amplitude, *n*-hexane, 260 K); upper part: simulated spectrum ($\langle g\rangle = 2.013$, $\langle a\rangle$ (^{31}P) = 3.6, 20.0, 32.6, 40.0, 80.0, and 84.0 G).

of **1** therefore stops the new formation of **1b**. Of course, the observed radical formation cannot fully prove the proposed radical reaction mechanism, but it gives evidence of a photolytic homolysis of **1**.

After the initial photochemical P–P bond breaking, a P–C bond dissociation and a radical recombination reaction might form a closed shell intermediate **1c** as shown in Scheme 9. The latter has the constitutional requirements for a twofold [2+2] cyclic addition reaction furnishing hexaphosphapentaprismane (**2**).

All structural and spectroscopic data of the three chiral cage compounds give clear evidence that only one pair of enantiomers is almost exclusively observable in the solid state as well as in solutions, in spite of the fact, that the number of stereogenic centers would allow the formation of many diastereomers. As the preparative access to key molecule **1** is based on achiral (**8**) or racemic (**6**, **7a**) starting materials with smaller numbers of stereogenic centers, the highly preferred formation of the two observed enantiomers of **1** must be based on a cascade of highly diastereoselective reaction steps. The same must be true for the rearrangement **1** → **2**. This is a very interesting feature of these cage compounds, and it seems to be a general one.[14]

Experimental Section

General considerations: All experiments were conducted under an inert atmosphere of nitrogen or argon by using standard Schlenk and cannula techniques. Solvents were dried according to described procedures[27] and used freshly distilled from the drying agent. Compound 1-trimethylstannyl-3,5-di(*tert*-butyl)-1,2,4-triphosphole (**7a**) was prepared as described previously[14] and distilled in an oil pump vacuum for purification. *tert*-Butylphosphaacetylene (**3**)[28] and the potassium triphospholyl anion (**8**)[15] were prepared as described in the literature. Iterative simulations of ^{31}P NMR spectra have been carried out using the programs g-NMR for Windows 4.1.0, Cherwell Scientific Publishing Ltd. 1997 (**2**) and Nuts 2D Version 5.084, and NMR Data Processing Program, Acorn NMR 1995 (**9**). Simulation of EPR spectra (**1b**) has been carried out using the program Simfonia from Bruker.

Tetra(*tert*-butyl)hexaphosphadecadiene tBu$_4$C$_4$P$_6$ (1), first method: A suspension of **5** in dichloromethane (15 mL) was prepared from $AlCl_3$ (2.22 g, 16.7 mmol) and *tert*-butylphosphaalkyne (**3**, 1.58 g, 15.8 mmol) as described in the literature.[13] The solvent and all volatile substances were removed in vacuo at 25 °C. The residue was suspended again in dichloromethane (10 mL). DMSO (1.39 mL) in dichloromethane (9 mL) was added slowly at −78 °C to the stirred suspension. After 15 minutes the solution was allowed to reach room temperature and was stirred for 36 hours. The solvents and all volatile substances were removed in vacuo, and the residue was extracted seven times with *n*-pentane (each 10 mL). Chromatographic workup on silica gel with *n*-pentane as eluent yielded **1** (0.27 g, 0.58 mmol, 22 %) as the second fraction. From *n*-pentane tufts of orange crystals were obtained.

Second method: All procedures were carried out under exclusion of light as far as possible. A sample of $[CrCl_3(thf)_3]$ (0.416 g, 1.110 mmol) was suspended in THF (30 mL). At −40 °C, [(η^1-tBu$_2$C$_2$P$_3$)Sn(Me)$_3$] (**7a**) (0.416 g, 1.089 mmol) in THF (20 mL) was added. The color of the mixture changed first to purple and later on to brown. After two hours, the solution was allowed to warm up and was stirred for half an hour at room temperature. The solvent and all volatile substances were removed in a vacuum. The residue was extracted with *n*-hexane (20 mL), the solution was filtered, and the solvent was removed in a vacuum again. The residue was purified by chromatography on silica gel/5 % H_2O with an *n*-hexane/toluene mixture (1:1) as eluent. The main orange fraction was collected to get **1** (314 mg, 0.68 mmol, 31 %) as a red solid.

Third method: All procedures were carried out under exclusion of light as far as possible. A sample of $HgCl_2$ (0.491 g, 1.8 mmol) was suspended in toluene (60 mL). At 0 °C, (η^1-tBu$_2$C$_2$P$_3$)(SnMe$_3$) **7a** (1.28 g, 3.45 mmol) in toluene (20 mL) was added. Immediately a red substance coagulated and redissolved. The reaction mixture was stirred for four hours at 0 °C. The volume of the solvent was reduced in vacuo to 10 mL, and the orange-gray residue was extracted several times with *n*-hexane. The orange solution was filtered, vacuum dried, and purified by chromatography on silica gel/5 % H_2O with a *n*-hexane/toluene mixture (1:1) as eluent. One orange fraction was collected. From *n*-hexane, **1** (601 mg, 1.30 mmol, 72 %) crystallized at −18 °C as thin intergrown plates.

Spectroscopic data for 1: M.p. 98 °C; ^1H NMR (269.71 MHz, C_6D_6, RT): $\delta = 1.34$ (d, ^3J(H,P) = 1.16 Hz, 9H; CH_3), 1.30 (d, ^3J(H,P) = 1.62 Hz, 9H; CH_3), 1.16 (s, 9H; CH_3), 1.07 (s, 9H; CH_3); $^{31}P\{^1H\}$ NMR (161.7 MHz, C_6D_6, 24 °C): $\delta = 357.4$ (dm, ^1J(P4,P6) = 315 Hz, 1P; P4), 352.6 (m, 1P; P2), 32 (ddd, ^1J(P4,P6) = 315, ^2J(P,P) = 32, ^2J(P,P) = 21 Hz, 1P; P6), 31.02 (dddd, $^{1\text{ or }2}J$(P,P) = 187, $^{1\text{ or }2}J$(P,P) = 149, ^2J(P,P) = 38, ^2J(P,P) = 21 Hz, 1P; P1, 3 or 5), 10.9 (ddd, $^{1\text{ or }2}J$(P,P) = 187, $^{1\text{ or }2}J$(P,P) = 131, ^2J(P,P) = 32 Hz, 1P; P1, 3 or 5), −13.4 (dd, $^{1\text{ or }2}J$(P,P) = 149, $^{1\text{ or }2}J$(P,P) = 131 Hz, 1P; P1, 3 or 5); ^{13}C NMR (100 MHz, C_6D_6, RT): $\delta = 236.9$ (each m, C5 and C7), 207.8, 81.8 (each m, C6 and C8), 76.3, 44.9 (dd, ^2J(C,P) = 21.9 and 10.5 Hz; $C(CH_3)_3$), 41.8 (pt, ^2J(C,P) = 15.3 Hz; $C(CH_3)_3$), 38.1 (dd, ^2J(C,P) = 15.3 and 11.4 Hz; $C(CH_3)_3$), 37.7 (m, $C(CH_3)_3$), 35.1 (br s, $C(CH_3)_3$), 33.6 (p quin, ^3J(C,P) = 7.6 and 5.7 Hz; $C(CH_3)_3$), 32.2 (d, ^3J(C,P) = 11.4 Hz; $C(CH_3)_3$), 32.0 (d, ^3J(C,P) = 8.6 Hz; $C(CH_3)_3$); MS (FD^+, *n*-hexane): *m*/*z* (%): 462 (100) [M^+]; MS (EI, 70 eV): *m*/*z* (%): 462 (97) [M^+], 400 (20) [$M^+ - 2P$], 362 (24) [M^+ − (PC–tBu)], 169 (100) [P^+(C–tBu)$_2$].

Tetra(*tert*-butyl)hexaphosphadecadiene tBu$_4$C$_4$P$_6$ (9): A sample of $[CrCl_3(thf)_3]$ (0.813 g, 2.17 mmol) was suspended in THF (40 mL). At −50 °C, (η^1-tBu$_2$C$_2$P$_3$)(SnMe$_3$) (**7a**) (0.864 g, 2.188 mmol) in THF (20 mL) was added. The mixture was allowed to warm up overnight to 8 °C and was stirred for half an hour at room temperature. Due to ^{31}P NMR analysis of the reaction mixture, tBu$_4$C$_4$P$_6$ **1**, tBu$_4$C$_4$P$_6$ **2**, tBu$_4$C$_4$P$_6$ **9**, and the partially hydrogenated P–C cage tBu$_4$C$_4$P$_6$H$_2$[29] were formed in the ratio 1:1.3:3.2:8.3.

Workup of ***9***: This involved cooling down the solution to −70 °C to precipitate most of the tBu$_4$C$_4$P$_6$H$_2$ as crystals, removing the THF in a vacuum, dissolving the residue in *n*-hexane, filtration, and chromatography on silica gel/5 % H_2O with *n*-hexane as eluent. The first yellowish green fraction yielded a mixture of tBu$_4$C$_4$P$_6$ **9** and hexaphosphachromocene [(η^5-tBu$_2$C$_2$P$_3$)$_2$Cr] (**10**) (92 mg). Repeated recrystallization led to a few crystals of pure **9**, which were suitable for X-ray diffraction.

Spectroscopic data for the mixture of 9 and NMR-silent 10: ^1H NMR (399.65 MHz, C_6D_6, 20.9 °C): $\delta = 1.48$ (s, 9H; CH_3), 1.35 (s, 9H; CH_3), 1.34 (s, 9H; CH_3), 1.32 (s, 9H; CH_3); $^{31}P\{^1H\}$ NMR (161.7 MHz, C_6D_6, 20.5 °C): $\delta = 339.7$ (1P; P2), 286.5 (1P; P5), 23.0 (1P; P4), −113.5 (1P; P3), −116.4 (1P; P1), −124.4 (1P; P6), simulated coupling constants: ^1J(P4,P6) = 240.3, ^1J(P3,P7) = 245.1, ^1J(P4,P3) = 296.4, ^2J(P2,P3) = 27.2, ^2J(P2,P1) = 21.7, ^2J(P2,P6) = 21.4, ^2J(P5,P4) = 6.4, ^2J(P5,P1) = −4.6, ^2J(P5,P6) = 11.4, ^2J(P4,P1) = −4.2, ^2J(P3,P5) = 37.4, ^2J(P1,P6) = 5.9, ^3J(P2,P4) = 19.7, ^3J(P5,P3) = 1.8, ^4J(P2,P5) = 2.5 Hz; the relative signs of the coupling constants were only unambiguous for those parts of the spectrum with

second-order couplings; $^{13}C\{^1H\}$ NMR (100.40 MHz, C_6D_6, 20.6 °C): $\delta =$ 44.5 (ddd, $^2J(C,P) = 3.2$, $^2J(C,P) = 23.8$, $^2J(C,P) = 27.0$ Hz; $C(CH_3)_3$), 43.7 (dd, $^2J(C,P) = 16.9$, $^2J(C,P) = 16.9$ Hz; $C(CH_3)_3$), 41.3 (ddd, $^2J(C,P) = 8.7$, $^2J(C,P) = 8.7$, $^2J(C,P) = 22.0$ Hz; $C(CH_3)_3$), 38.9 (ddd, $^2J(C,P) = 14.2$, $^2J(C,P) = 14.2$, $^2J(C,P) = 8.7$ Hz; $C(CH_3)_3$), 33.3 (ddd, $^3J(C,P) = 8.2$, $^3J(C,P) = 8.2$, $^3J(C,P) = 8.2$ Hz; $C(CH_3)_3$), 32.7 (dd, $^3J(C,P) = 9.6$, $^3J(C,P) = 16.1$ Hz; $C(CH_3)_3$), 32.2 (dd, $^3J(C,P) = 6.8$, $^3J(C,P) = 14.2$ Hz; $C(CH_3)_3$), 30.9 (ddd, $^3J(C,P) = 6.4$, $^3J(C,P) = 6.4$, $^3J(C,P) = 12.9$ Hz; $C(CH_3)_3$); the signals of the skeletal C atoms were not detected; MS (FD^+, *n*-hexane): *m*/*z* (%): 462 (100) [tBu$_4$C$_4$P$_6^+$], 514 (65) [tBu$_4$C$_4$P$_6$Cr$^+$].

Tris[tetra(*tert*-butyl)hexaphosphadecyl mercury] [(tBu$_4$C$_4$P$_6$)Hg]$_3$ (11): A solution of $HgCl_2$ (0.454 g, 1.6 mmol) in THF (20 mL) was added to [K(tBu$_2$C$_2$P$_3$)] (**8**, 0.9 g, 3.3 mmol) in THF (20 mL) at −40 °C. The temperature of the mixture was allowed to slowly rise to room temperature. It was stirred overnight to afford a yellow suspension. The solvent was filtered off, and the yellow powder extracted with chloroform to give a very light-sensitive solution. After removal of the solvent in vacuo, [(tBu$_4$C$_4$P$_6$)Hg]$_3$ (**11**) (0.5 g, 0.25 mmol, 47%) was obtained as a yellow powder.

Spectroscopic data for 11: ^1H NMR (300 MHz, $CDCl_3$, 25 °C): $\delta = 1.30$ (s, 27H), 1.27 (s, 27H), 1.22 (s, 27H), 1.15 (s, 27H); $^{31}P\{^1H\}$ NMR (121.68 MHz, $CDCl_3$, 25 °C, all signals were complex multiplets due to only partially resolved long-range P–P coupling, the multiplicity given deals with the dominant ^1J(P,P), only see Figure 6): $\delta = 179.9$ (s, P4), 145.7 (s, P5), 104.5 (d, ^1J(P,P) = 285 Hz; P3), 74.1 (d, ^1J(P,P) = 269 Hz; P6), 11.4 (d, ^1J(P,P) = 269 Hz; P1), −65.3 (d, ^1J(P,P) = 285 Hz; P2).

Bis[3,5-di(*tert*-butyl)-1,2,4-triphospholyl]mercury (η^1-π-tBu$_2$C$_2$P$_3$)$_2$Hg (12): $HgCl_2$ (0.177 g, 0.65 mmol) was dissolved in diethyl ether (7 mL). At −80 °C, (η^1-tBu$_2$C$_2$P$_3$)(SnMe$_3$) (**7a**, 0.489 g, 1.24 mmol) in diethyl ether (10 mL) was added. Immediately a red solid coagulated. The mixture was allowed to warm up to −30 °C with exclusion of light. The solid precipitated, and the diethyl ether was removed by syringe. The residue was washed several times with diethyl ether at 0 °C to remove $HgCl_2$ and [$SnCl(Me)_3$]. The solvent was evaporated in a stream of nitrogen gas, and product **12** (411 mg, 0.62 mmol, 95%) was dried in vacuo to yield a dark red amorphous solid.

Spectroscopic data for 12: IR (KBr): $\tilde{\nu} = 2953$ (s, (CH)), $\delta_{as} = 1460$ (m, ($C(CH_3)_3$)), 1457 (m), $\delta_{sy} = 1385$ (s, ($C(CH_3)_3$)), 1361 (s), $\tilde{\nu} = 1111$ (br s, (C=P)), $\tilde{\nu} = 802$ cm^{-1} (m, (C–P)); CP MAS ^{31}P NMR (202.35 MHz, RT): $\delta = 297, 161$. To identify the isotropic signals, the measurement was carried out at three different rotation frequencies (4185, 5280, and 6526 Hz). The product was insoluble in DMSO or water and stable for several days at least. In diethyl ether it decomposed within days at room temperature, and mercury was eliminated. In acetone or methanol, the decomposition took a few hours, in toluene or *n*-hexane, **12** decomposed nearly immediately.

Tetra(*tert*-butyl)hexaphosphapentaprismane tBu$_4$C$_4$P$_6$ (2); first method: The starting material **1** was prepared from **5** and DMSO. A solution of **1** (0.05 g, 0.11 mmol) in C_6D_6 (0.5 mL) was exposed to diffuse daylight and stirred for two days at room temperature. By slowly cooling the solution down to 8 °C, compound **2** (20 mg, 0.043 mmol, 40%) was obtained after about 24 hours as orange needles.

Second method: The starting material **1** was prepared by the second method from [$CrCl_3$(thf)$_3$] and **7a** without the concluding column chromatography. Crude **1** (243 mg, ≤0.526 mmol) was dissolved *n*-hexane (20 mL). The solvent was removed by reduced pressure to produce a thin film of **1** on the glass surface. The film was exposed to the usual laboratory light for two hours and was dissolved in a small amount of *n*-hexane. At −18 °C, **2** (98 mg, 0.212 mmol, 40%) crystallized.

Third method: $HgCl_2$ (0.15 g, 0.5 mmol) in THF (10 mL) was added to [K(tBu$_2$C$_2$P$_3$)] (0.3 g, 1.1 mmol) in THF (10 mL) at −40 °C, and then the temperature was allowed to rise to room temperature. The color of the solution initially changed to red brown. While stirring for 24 hours an orange solution was formed slowly, and mercury precipitated. The solvent was removed in vacuo, and the residue extracted with toluene. Compound **2** (50 mg, 0.11 mmol, 20%) was isolated as orange crystals by recrystallization from toluene at −40 °C.

Spectroscopic data for 2: M.p. 188 °C; ^1H NMR (399.65 MHz, $CDCl_3$, 22.5 °C): $\delta = 1.28$ (s, 18H; CH_3), 1.21 (s, 18H; CH_3); $^{31}P\{^1H\}$ NMR (161.7 MHz, $CDCl_3$, 24.7 °C): $\delta = 241.9$ (2P; P(Y+Y′) = P1,P6), 178.1 (2P; P(X+X′) = P1,P4), [AA′XX′YY′] spin system, −3.78 (2P; P(A+A′) = P1,P4), simulated coupling constants: ^1J(PA,PA′) = 63.74, ^1J(PA,PX) = −86.42, ^2J(PA,PY) = 33.33, ^2J(PA,PX′) = 4.46, ^3J(PA,PY′) = 3.56, ^3J(PX,PX′) = 5.99, ^2J(PX,PY) = −3.80, ^2J(PX,PY′) = 29.55, ^2J(PY,PY′) = −6.74 Hz; $^{13}C\{^1H\}$ NMR (100.4 MHz, $CDCl_3$, 24.9 °C): $\delta =$ 128.83 (d, ^1J(P,P) = 83.4 Hz; $C_{skeletal}$), 128.00 (t, ^1J(P,P) = 24.0 Hz; $C_{skeletal}$), 36.47 (m, $C(CH_3)$), 32.64 (m, $C(CH_3)$), 27.26 (m, $C(CH_3)$), 25.41 (m, $C(CH_3)$).

[Tetra(*tert*-butyl)hexaphosphadecadiene]bis(pentacarbonyl)tungsten (tBu$_4$C$_4$P$_6$)[W(CO)$_5$]$_2$ (13): [$W(CO)_6$] (101 mg, 0.29 mmol) was dissolved in THF (60 mL) and irradiated in a pyrex glass apparatus with a 125 W high-pressure mercury lamp for 25 minutes. Compound **1** (60 mg, 0.13 mmol) in THF (5 mL) was added, and the solution was stirred for five hours at room temperature. The solvent was removed in vacuo. The residue was purified by chromatography on silica gel with pentane as eluent. After a first yellow run, the second orange red fraction was collected and recrystallized from *n*-pentane to yield binuclear complex **13** (67 mg, 0.06 mmol, 46%).

Spectroscopic data for 13: M.p. 156 °C (decomp); ^1H NMR (400 MHz, C_6D_6, 75 °C): $\delta = 1.47$ (s, 9H; CH_3), 1.42 (s, 9H; CH_3), 1.29 (s, 9H; CH_3), 1.07 (s, 9H; CH_3); $^{31}P\{^1H\}$ NMR (81 MHz, C_6D_6, RT): $\delta = 355.8$ (1P; P5), 281.6 (1P; P8), 56.9 (1P; P2), 56.8 (1P; P7), 30.0 (1P; P1), −1.9 (1P; P3), simulated coupling constants: ^1J(P7,P8) = 366.5, ^1J(P2,P1) = 201.0, ^1J(P2,P3) = 183.1, ^2J(P1,P3) = 109.0, ^2J(P1,P8) = 56.6, ^2J(P5,P7) = 29.8, ^2J(P2,P5) = 19.0, ^2J(P3,P7) = 16.0, ^2J(P2,P7) = 13.4, ^3J(P2,P8) = 11.0 Hz, ^3J(P3,P5) = 8.9, ^1J(P8,^{183}W) = 252.9 Hz; MS (EI, 70 eV): 1110 (7) [M^+], 1082 (14) [M^+ − CO], 231 (100) [P^+(PC–tBu)$_2$]; elemental analysis calcd (%) for $C_{30}H_{36}O_{10}P_6W_2$ (1110.11): C 32.46, H 3.27; found: C 32.67, H 3.32.

Crystal structure determination of 1 and 9: Intensity data were collected on a Siemens P4 diffractometer (ω-scan technique, 6.0° min^{-1}, $Mo_{K\alpha}$ radiation, graphite monochromator, $\lambda = 0.71073$ Å) at 200 K by using the XSCAnS 2.20 software.[30] All data were corrected for Lorentz and polarization effects. For **1**, absorption effects have been corrected by using ψ scans ($T_{min} = 0.449$, $T_{max} = 0.517$), while for **9**, absorption effects have been neglected. The structures were solved by direct methods and refined by the full-matrix least-squares method against F^2 with all reflections using SHELXTL programs.[31] All non-hydrogen atoms were refined anisotropically. For **1**, the crystal under study proved to be an inversion twin with the twin component ration 0.5. All hydrogen atoms of **1** were geometrically positioned with isotropic displacement parameters 1.5 times the equivalent isotropic displacement parameter of the adjacent carbon atom. In the case of **9**, the positions of all hydrogen atoms were taken from a difference Fourier synthesis, and their positional parameters were defined with a fixed common isotropic displacement parameter. Crystal data and experimental details are listed in Table 5.

Crystal structure determination of 2: Crystal data were collected on a Bruker AXS SMART 1000 diffractometer with a CCD area detector ($Mo_{K\alpha}$ radiation, graphite monochromator, $\lambda = 0.71073$ Å) at −100 °C by using the SMART software.[32] The reflection intensities were integrated by using SAINT[32] and corrected for absorption by using SADABS.[33] The structures were solved by direct methods and refined by the full-matrix least-squares method against F^2 with all reflections by using SHELXTL programs.[34] All non-hydrogen atoms were refined anisotropically. All hydrogen atoms were located in difference Fourier maps and refined isotropically. Crystal data and experimental details are listed in Table 6.

Crystal structure determination of 11: Crystal data were collected on a KappaCCD area detector with $\lambda = 0.71073$ Å at 173(2)K. The structure was solved and refined with the SHELX-97 suite of programs by using the WinGX interface. A multiscan absorption correction was applied, and the structure was refined by using the full-matrix least-squares method on F^2. Crystal data and experimental details are listed in Table 6.

Crystal structure determination of 13: Crystal data were collected on a STOE-Imaging Plate Diffraction System at 293 K ($Mo_{K\alpha}$ radiation, graphite monochromator, $\lambda = 0.71073$ Å). The structure was solved by direct methods and refined by the full-matrix least-squares method against F^2 by using SHELXS-86 and SHELXL-93. All non-hydrogen atoms were refined anisotropically. Crystal data and experimental details are listed in Table 9.

CCDC-163467 (**1**), CCDC-163468 (**2**), CCDC-163469 (**9**), CCDC-163470 (**11**), and CCDC-163471 (**13**) contain the supplementary crystallographic data for this paper. These data can be obtained free of charge via www.ccdc.cam.ac.uk/conts/retrieving.html (or from the Cambridge Crys-

  0947-6539/02/0811-2632 $ 20.00+.50/0 *Chem. Eur. J.* **2002**, *8*, No. 11

tallographic Data Centre, 12 Union Road, Cambridge CB21EZ, UK; fax: (+44) 1223-336-033; or e-mail: deposit@ccdc.cam.ac.uk).

Acknowledgements

This work was supported by the Deutsche Forschungsgemeinschaft and the Fonds der Chemischen Industrie. M.Z. is grateful for a scholarship by the DFG-Graduiertenkolleg P*hosphorchemie als Bindeglied verschiedener chemischer Disziplinen*, at the University of Kaiserslautern, Germany. J.F.N. and M.D.F. thank EPSRC for research funding, and M.M.A.-K. acknowledges the Atomic Energy Commission of Syria for a scholarship.

[1] T. J. Katz, N. Acton, *J. Am. Chem. Soc.* **1973**, *95*, 2738.
[2] P. E. Eaton, T. W. Cole, *J. Am. Chem. Soc.* **1964**, *86*, 3157.
[3] a) P. E. Eaton, Y. S. Or, S. J. Branca, *J. Am. Chem. Soc.* **1981**, *103*, 2134; b) P. E. Eaton, Y. S. Or, S. J. Branca, B. K. R. Shankar, *Tetrahedron* **1986**, *42*, 1621.
[4] K. B. Dillon, F. Mathey, J. F. Nixon, *Phosphorus, The Carbon Copy*, Wiley, Chichester, **1998**.
[5] For reviews see: a) M. Regitz, P. Binger, *Angew. Chem.* **1988**, *100*, 1541; *Angew. Chem. Int. Ed. Engl.* **1988**, *27*, 1484; b) M. Regitz, *Chem. Rev.* **1990**, *90*, 191; c) M. Regitz, P. Binger in *Multiple Bonds and Low Coordination in Phosphorus Chemistry* (Eds.: M. Regitz, O. J. Scherer), Thieme, Stuttgart, **1990**, p. 58; d) J. F. Nixon, *Coord. Chem. Rev.* **1995**, *145*, 201; e) A. Mack, M. Regitz, *Chem. Ber./Recl.* **1997**, *130*, 823.
[6] a) A. Mack, M. Regitz, *Chem. Ber./Recl.* **1997**, *130*, 823; b) A. Mack, B. Breit, T. Wettling, U. Bergsträßer, S. Leininger, M. Regitz, *Angew. Chem.* **1997**, *109*, 1396; *Angew. Chem. Int. Ed. Engl.* **1997**, *36*, 1337; c) B. Geißler, T. Wettling, S. Barth, P. Binger, M. Regitz, *Synthesis* **1994**, 1337; d) M. Regitz, A. Hoffmann, U. Bergsträßer in *Modern Acetylene Chemistry* (Eds.: P. J. Stang, F. Diederich), VCH, New York, **1995**, p. 173; e) T. Wettling, PhD thesis, University of Kaiserslautern (Germany), **1990**.
[7] a) T. Wettling, J. Schneider, O. Wagner, C. G. Kreiter, M. Regitz, *Angew. Chem.* **1989**, *101*, 1035; *Angew. Chem. Int. Ed. Engl.* **1989**, *28*, 1013; b) S. M. Bachrach, L. M. Periott, *Tetrahedron Lett.* **1993**, *34*, 6365; c) R. Gleiter, K. H. Pfeifer, M. Baudler, G. Scholz, T. Wettling, M. Regitz, *Chem. Ber.* **1990**, *123*, 757; d) J.-L. M. Abboud, H. Herreros, R. Notario, O. Mó, M. Yáñez, M. Regitz, J. Elguero, *J. Org. Chem.* **1996**, *61*, 7813; e) M. Birkel, J. Schulz, U. Bergsträßer, M. Regitz, *Angew. Chem.* **1992**, *104*, 870; *Angew. Chem. Int. Ed. Engl.* **1992**, *31*, 879.
[8] a) P. Binger, R. Milczarek, R. Mynott, E. Raabe, C. Krüger, M. Regitz, *Angew. Chem.* **1986**, *98*, 645; *Angew. Chem. Int. Ed. Engl.* **1986**, *56*, 644; b) P. B. Hitchcock, M. J. Maah, J. F. Nixon, *J. Chem. Soc. Chem. Commun.* **1986**, 737; c) P. Binger, B. Biedenbach, R. Schneider, M. Regitz, *Synthesis* **1989**, 960; d) P. Binger, B. Biedenbach, R. Mynott, C. Krüger, P. Betz, M. Regitz, *Angew. Chem.* **1988**, *100*, 1219; *Angew. Chem. Int. Ed. Engl.* **1988**, *27*, 1157; e) T. Wettling, G. Wolmershäußer, P. Binger, M. Regitz, *J. Chem. Soc. Chem. Commun.* **1990**, 1541; f) P. Binger, G. Glaser, S. Albus, C. Krüger, *Chem. Ber.* **1995**, *128*, 1261; g) P. Binger, B. Biedenbach, C. Krüger, M. Regitz, *Angew. Chem.* **1987**, *99*, 798; *Angew. Chem. Int. Ed. Engl.* **1987**, *26*, 764; h) R. Milczarek, W. Rüssler, P. Binger, K. Jonas, K. Angermund, C. Krüger, M. Regitz, *Angew. Chem.* **1987**, *99*, 957; *Angew. Chem. Int. Ed. Engl.* **1987**, *26*, 908; i) P. Binger, S. Leininger, J. Stannek, B. Gabor, R. Mynott, J. Bruckmann, C. Krüger, *Angew. Chem.* **1995**, *107*, 2411; *Angew. Chem. Int. Ed. Engl.* **1995**, *34*, 2227; j) F. Tabellion, A. Nachbauer, S. Leininger, C. Peters, F. Preuss, M. Regitz, *Angew. Chem.* **1998**, *110*, 1318; *Angew. Chem. Int. Ed.* **1998**, *37*, 1233; k) P. Binger, G. Glaser, B. Gabor, R. Mynott, *Angew. Chem.* **1995**, *107*, 114; *Angew. Chem. Int. Ed. Engl.* **1995**, *34*, 81; l) L. Weber, *Adv. Organomet. Chem.* **1997**, *41*, 1.
[9] a) B. Geißler, T. Wettling, S. Barth, P. Binger, M. Regitz, *Synthesis* **1994**, 1337; b) T. Wettling, B. Geißler, R. Schneider, S. Barth, P. Binger, M. Regitz, *Angew. Chem.* **1992**, *104*, 761; *Angew. Chem. Int. Ed. Engl.* **1992**, *31*, 786; c) B. Geißler, S. Barth, U. Bergsträßer, M. Slany, J. Durkin, P. B. Hitchcock, M. Hofmann, P. Binger, J. F. Nixon, P. von Ragué Schleyer, M. Regitz, *Angew. Chem.* **1995**, *107*, 485; *Angew. Chem. Int. Ed. Engl.* **1995**, *34*, 484.
[10] R. Bartsch, J. F. Nixon, P. B. Hitchcock, *J. Organomet. Chem.* **1989**, *375*, C31.
[11] V. Caliman, P. B. Hitchcock, J. F. Nixon, P. v. R. Schleyer, *Angew. Chem.* **1994**, *106*, 2284; *Angew. Chem. Int. Ed. Engl.* **1994**, *33*, 2202.
[12] a) D. Hu, H. Schäufele, H. Pritzkow, U. Zenneck, *Angew. Chem.* **1989**, *101*, 929; *Angew. Chem. Int. Ed. Engl.* **1989**, *28*, 900; b) D. Böhm, D. Hu, U. Zenneck, *Phosphorus Sulfur Silicon Relat. Elem.* **1993**, *77*, 5.
[13] a) B. Breit, U. Bergsträßer, G. Maas, M. Regitz, *Angew. Chem.* **1992**, *104*, 1043; *Angew. Chem. Int. Ed. Engl.* **1992**, *31*, 1055; b) B. Breit, M. Regitz, *Chem. Ber.* **1996**, *129*, 489.
[14] A. Elvers, F. W. Heinemann, B. Wrackmeyer, U. Zenneck, *Chem. Eur. J.* **1999**, *5*, 3143.
[15] Ch. Callaghan, G. K. B. Clentsmith, F. G. N. Cloke, P. B. Hitchcock, J. F. Nixon, D. M. Vickers, *Organometallics* **1999**, *18*, 793.
[16] R. Bartsch, P. B. Hitchcock, J. F. Nixon, *J. Organomet. Chem.* **1988**, *356*, C1.
[17] M. D. Francis, P. B. Hitchcock, J. F. Nixon, *Chem. Commun.* **2000**, 2026.
[18] J. J. Durkin, M. D. Francis, P. B. Hitchcock, C. Jones, J. F. Nixon, *J. Chem. Soc. Dalton Trans.* **1999**, 4057; A. Elvers, PhD thesis, Unversität Erlangen, Nürnberg (Germany), **1998**; J. J. Durkin, PhD thesis, University of Sussex (UK), **1996**.
[19] J. J. Durkin, M. D. Francis, P. B. Hitchcock, C. Jones, J. F. Nixon, *J. Chem. Soc. Dalton Trans.* **1999**, 4057; S. J. Black, M. D. Francis, C. Jones, *Chem. Commun.* **1997**, 305.
[20] a) F. H. Allen, O. Kennard, D. G. Watson, L. Brammer, A. G. Orpen, R. Tayler, *J. Chem. Soc. Perkin Trans.* **1987**, *2*, 1; b) *CRC Handbook of Chemistry and Physics*, 77th ed., (Ed.: D. R. Lide), CRC Press, Boca Raton, **1996–1997**, p. 9.
[21] a) N. N. Greenwood, A. Earnshaw, *Chemie der Elemente*, VCH, Weinheim, **1988**, p. 618; b) D. E. C. Corbridge, *The Structural Chemistry of Phosphorus*, Elsevier, Amsterdam, **1974**.
[22] N. Korber, J. Daniels, H. G. von Schnering, *Angew. Chem.* **1996**, *108*, 1188; *Angew. Chem. Int. Ed. Engl.* **1996**, *35*, 1107.
[23] M. M. Al-Ktaifani, D. P. Chapman, M. D. Francis, P. B. Hitchcock, J. F. Nixon, L. Nyulaszi, *Angew. Chem.* **2001**, *113*, 3582; *Angew. Chem. Int. Ed.* **2001**, *40*, 3474.
[24] S. Berger, S. Braun, H.-O. Kalinowski, *NMR-Spektroskopie von Nichtmetallen*, *Vol. 3*: ^{31}P-*NMR-S*pektroskopie, Thieme, Stuttgart, **1993**, p. 15.
[25] S. Berger, S. Braun, H.-O. Kalinowski, *NMR-Spektroskopie von Nichtmetallen*, *Vol. 3*: *^{31}P-NMR-S*pektroskopie, Thieme, Stuttgart, **1993**, p. 152.
[26] a) A. Marinetti, S. Bauer, L. Ricard, F. Mathey, *Organometallics* **1990**, *9*, 793; b) P. B. Hitchcock, C. Jones, J. F. Nixon, *J. Chem. Soc. Chem. Commun.* **1995**, 2167; c) T. W. Mackewitz, D. Ullrich, U. Bergsträßer, S. Leininger, M. Regitz, *Liebigs Ann./Recl.* **1997**, 1827.
[27] D. D. Perrin, W. L. F. Armarego, *Purification of Laboratory Chemicals*, 3rd ed., Butterworth-Heinemann, Oxford, **1988**.
[28] W. Rösch, T. Allspach, U. Bergsträßer, M. Regitz in *Synthetic Methods of Organometallic and Inorganic Chemistry*, *Vol. 3* (Ed.: H. H. Karsch), Thieme, Stuttgart, **1996**, p. 11.
[29] R. Bartsch, P. B. Hitchcock, J. F. Nixon, *J. Chem. Soc. Chem. Commun.* **1989**, 1046.
[30] Siemens Analytical X-Ray Instruments, Inc., Madison, WI, **1996**.
[31] SHELXTL NT 5.1, Bruker AXS, Inc., Madison, WI, **1998**.
[32] SMART and SAINT, NT V5.0, Area Detector Control and Integration Software, Bruker AXS, Madison, WI, **1999**.
[33] G. M. Sheldrick, SADABS, Program for Scaling and Correction of Area Detector Data, Göttingen, **1996**.
[34] G. M. Sheldrick, SHELXTL NT V5.1, Bruker AXS, Madison, WI, **1999**.

Received: July 17, 2001
Revised: February 14, 2002 [F3422]